IBRACON Structures and Materials Journal
Revista IBRACON de Estruturas e Materiais
ISSN 1983-4195 ismj.org

ORIGINAL ARTICLE

Mix design of eco-efficient high-strength mortars optimized by the compressible packing model

Dosagem de argamassas de alta resistência ecoeficientes otimizadas pelo modelo de empacotamento compressível

Nicolle Talyta Arriagada Soto[a]
Gustavo Macioski[a]
Juarez Hoppe Filho[b]
Nayara Soares Klein[a]

[a]Universidade Federal do Paraná – UFPR, Curitiba, PR, Brasil
[b]Universidade Federal do Oeste da Bahia – UFOB, Barreiras, BA, Brasil

Received 25 April, 2023
Revised 15 December, 2023
Accepted 19 January, 2024

Abstract: The production of eco-efficient cement-based materials is essential to reduce CO_2 emissions from the construction industry. A substantial reduction in global CO_2 emissions can be achieved by using clinker in mortar and concrete more efficiently and using low-CO_2 minerals as partial replacements for Portland cement. However, the proportioning of eco-efficient composites is complex and the reduction in clinker content may affect its properties. This paper aims to optimize the mix design of high-strength mortars containing supplementary cementitious materials (limestone filler, fly ash, metakaolin, silica fume). The compressible packing model associated with a simplex mixture design were used together with chemical parameters, to limit the amount of active SCMs for the model iterations. The results show a significant decrease in the environmental impact of the mortars, which presented compressive strengths between 76 and 118 MPa at 91 days and binder indexes between 10 and 15 kg/m^3/MPa. The reactivity of the SCMs (based on the modified Chapelle test) were successfully used to establish the Portland cement substitution (up to 13%), preventing the presence of unreacted SCMs and optimizing the use of limestone filler and sand, which have a lower environmental impact. The high-performance blends reached 8.73 kg CO_2e/MPa, up to a 30% reduction in CO_2e emissions compared to the mortar with only Portland cement.

Keywords: carbon emission, supplementary cementitious materials, particle packing, eco-efficiency, simplex.

Resumo: A produção de materiais ecoeficientes à base de cimento é essencial para reduzir as emissões de CO_2 na indústria da construção civil. Pode-se alcançar reduções importantes nas emissões globais de CO_2 pelo uso mais eficiente do clínquer em argamassas e concretos, e pela utilização de adições minerais de baixo teor de CO_2 como substitutos parciais do cimento Portland. No entanto, a dosagem de compósitos ecoeficientes é complexa e a redução do teor de cimento pode afetar suas propriedades. Este artigo tem como objetivo otimizar a dosagem de argamassas contendo adições minerais (fíler de calcário, cinza volante, metacaulim, sílica ativa). O modelo de empacotamento compressível associado a um planejamento de mistura simplex foi utilizado juntamente com parâmetros químicos, para limitar a quantidade de adições minerais reativas para as iterações do modelo. Os resultados mostram uma redução significativa no impacto ambiental das argamassas, que apresentaram resistências à compressão entre 76 e 118 MPa aos 91 dias e índices de ligante entre 10 e 15 kg/m^3/MPa. A reatividade das adições minerais (baseada no teste de Chapelle modificado) foi utilizada com sucesso para estabelecer a substituição do cimento Portland (até 13%), evitando a presença de adições minerais sem reagir e otimizando o uso de fíler calcário e areia, que apresentam menor impacto ambiental. As misturas de alto desempenho atingiram 8,73 kg CO_2e/MPa, redução de até 30% nas emissões de CO_2 comparativamente às argamassas contendo apenas cimento Portland.

Palavras-chave: emissões de carbono, material cimentício suplementar, empacotamento de partículas, ecoeficiência, simplex.

How to cite: N. T. A. Soto, G. Macioski, J. Hoppe Filho, and N. S. Klein, "Mix design of eco-efficient high-strength mortars optimized by compressible packing model", *Rev. IBRACON Estrut. Mater.*, vol. 17, no. 6, e17611, 2024, https://doi.org/10.1590/S1983-41952024000600011

Corresponding author: Nicolle Talyta Arriagada Soto. E-mail: nicolle.a.soto@gmail.com
Financial support: None.
Conflict of interest: Nothing to declare.
Data Availability: The data that support the findings of this study are available from the corresponding author, N. T. A. Soto, upon reasonable request.

This is an Open Access article distributed under the terms of the Creative Commons Attribution License, which permits unrestricted use, distribution, and reproduction in any medium, provided the original work is properly cited.

1 INTRODUCTION

Cement remains the most consumed building material [1]: in 2019, 4.08 billion tons of cement were produced worldwide [2]. With this, it is estimated that for each person, around 535 kg of cement is consumed annually. Cement is the third largest energy-consuming industry accounting for 7% of the world's total CO_2 emissions [3]. The Intergovernmental Panel on Climate Change has estimated that to limit the increase in global temperature by up to 1.5°C, CO_2 emissions by 2030 must be reduced by 45%, and should reach 100% reduction by 2050 [4]. However, there is no downward trend in cement manufacturing [5], and there are prospects for an increase in world cement production of 12 to 23% by 2050 [6].

Some measures to reduce greenhouse gas emissions have been taken in cement plants, such as using more efficient furnaces and alternative fuels, reducing the proportion of clinker in cement, recapturing excess thermal energy and carbon capture [6]. However, it is considered unlikely that manufacturing process improvements will occur at the speed and intensity required to meet emissions reduction targets [7]. The reason is that only one-third of cement-related emissions are tied to fuel combustion, with the other two-thirds released in the decarbonization of limestone [6].

The alternatives for CO_2 reduction by the cement industry have been studied and developed on different fronts: (A) reducing concrete consumption for new structures by using high-strength concretes, it is possible to achieve the expected mechanical performance with smaller volumes of concrete [3]; (B) the use of supplementary cementitious materials (SCMs) in the production of more sustainable concretes allows a reduction in cement clinker percentage [8]. The goal is a global decrease in the percentage of clinker in cement from 0.65 (2014) to 0.60 by 2050 [6]. Although certain SCMs are by-products of other production chains, emissions related to their handling, grinding, and transportation should be accounted [9], hence, they do not reach the concrete with zero environmental impact, as seen in Table 1.

Table 1 - CO_2 emissions from construction materials (compiled from [10]-[12])

Material	CO_2 emission* (kg CO_2/kg material)
Clinker	0.830
Portland cement (clinker + gypsum)	0.860
Limestone filler	0.008
Calcinated clay/metakaolin	0.350
Fly ash	0.029
Slag	0.085
Silica fume	0.014
Fine aggregate	0.002
Coarse aggregate	0.003
Superplasticizer chemical admixture	0.767

*No transport considered

Most of the current production of SCMs is already employed by the cement industry [11]. The forecast is that the production of these materials in the coming years will only partially meet the demand [13]. The incorporation of SCMs without or with low reactivity, such as limestone filler, becomes one of the most promising alternatives in mitigating CO_2 emissions by the concrete industry. Its use does not require high investment since there is no need for calcination, and the availability is quite wide [13].

Despite the environmental appeal of using high volumes of SCMs, pozzolanic reactions depend on calcium hydroxide (portlandite) availability from the cement hydration. Its use in amounts that require more portlandite than is available from the cement causes part of the SCMs not to react, preventing the formation of hydrated phases. It could also delay the reaction due to the grain being coated with hydrated minerals, which slows down the step-retreat process [14], [15]. The presence of unreacted SCMs can yet become the origin of deleterious reactions in the future due to their unreacted glassy fraction or the release of alkalis in the pore solution [16]. Thus, the pozzolanic potential of reactive SCMs should be better explored, which depends on their chemical composition and physical characteristics. For this reason, when determining the percentages of cement to be replaced by SCMs, their degree of reactivity and the availability of calcium hydroxide should be considered to minimize the presence of unreactive SCMs. This chemical consideration is not usually taken in the mix design, but it can be incorporated in the design of eco-efficient cement composites, as proposed in this study, to optimize the use of SCMs.

Additionally, the use of particle packing techniques can also lead to a reduction on the cement content in concretes and mortars [17]–[19]. Its use combined with third-generation chemical admixtures reduces the amount of water in the mixture, ensuring a better filling of voids and densifying the cementitious matrix [20]. Sometimes, results obtained from the packing model suggest the use of an excessive amount of SCMs. Although it will help to increase the packing density, it prevents the presence of a minimum amount of Portland cement that is required for the pozzolanic reactions to take place or for the blend to achieve a minimum compressive strength.

The compressible packing model (CPM) is complex and requires several iterations to evaluate the maximum possible packing density. Therefore, the association of the particle packing theory with a simplex mixture design will require way less numerical processing, simplifying the use of the CPM and optimizing the mix design analysis. This approach for the application of particle packing theories could not be found in the literature and will be further explored in this paper.

Thus, this paper aims to optimize the mix design of high-strength mortars containing SCMs (limestone filler, fly ash, metakaolin, silica fume) through the compressible packing model. This paper's novelty lies in using chemical parameters to limit the amount of SCMs for the model iterations. The association of the CPM with a simplex mixture design to simplify the application of the particle packing model is also a new approach, which can be disseminated in producing eco-efficient cement composites.

2 PARTICLE PACKING THEORY

Particle packing can be defined as a method for selecting the best proportion between the granular materials. It seeks to fill the larger voids with smaller particles, thus obtaining a system with a significant decrease in the volume of voids [21], [22]. Besides being a valuable tool for proportioning aggregate fractions, some packing models allow the mix-design of concrete with fine particles (<125 μm) [23] and can be used for the development of pastes, mortars, grouts, and concretes. However, when it comes to fine particles, special attention must be paid to agglomeration, which is caused by cohesion forces between the grains. Forces such as Van der Walls, electrostatic charges, and chemical bonds are dominant in systems composed with fine particles. Due to their small size, low mass and large surface area, these interparticle forces overcome the effect of gravity and shear forces, which can separate the grains, and this effect causes the particles to agglomerate [21], [24], [25].

The studies of particle packing began with researchers trying to optimize particle size distribution curves of aggregates. This continuous approach of packing models was proposed by Füller and Thompson (1907), Andreasen and Andersen (1930) and Funk and Dinger (1980) [26]. On the other hand, discrete models that consider the packing of particles of two different sizes were developed by Furnas [27], Toufar and modified Toufar [28] and Dewar [29]. The linear packing model [30] allowed using several classes of particle sizes, considering the geometric interaction between these particles: the so-called wall effect and loosening effect. The compressible packing model (CPM) is an extension of the linear packing model, which added the consideration of the compaction index (K) when calculating the particle packing [31].

In a mixture of grains of different classes, where the grain sizes $d_1 > \cdots > d_i > \cdots > d_n$, one can say that class "i" is dominant if it ensures the continuity of the granular body. The maximum packing is reached when the smaller grains fill the empty spaces left by the larger grains. However, there are cases in which the interaction between the particles decreases the compactness of the mixture. These configurations, known as wall effect (a_{ij}) and loosening effect (b_{ij},), occur in granular classes of relatively close sizes and can be calculated by Equations 1 and 2 [31], where d_i is the particle dimension under consideration, and d_j corresponds to the dimension of the particle that is causing interference.

$$a_{ij} = \sqrt{1 - \left(1 - \frac{d_j}{d_i}\right)^{1,02}} \tag{1}$$

$$b_{ij} = 1 - \left(1 - \frac{d_i}{d_j}\right)^{1,50} \tag{2}$$

The virtual packing density (γ_i) of a polydisperse mixture containing "n" classes, is given in Equation 3 [31], where β_i and β_j correspond to the experimentally determined packing density of each size class and y_j is the volumetric proportion of class "i".

$$\gamma_i = \left(\frac{\beta_i}{1 - \sum_{j=1}^{i-1} \left[1 - \beta_i + b_{ij} \cdot \beta_i \left(1 - \frac{1}{b_j} \right) \right] \cdot y_j - \sum_{j=i+1}^{n} \left[1 - a_{ij} \cdot \frac{\beta_i}{\beta_j} \right] \cdot y_j} \right) \quad (3)$$

Equation 3 should be calculated considering each of the "n" classes as dominant, and the virtual packing density of the mixture will be the smallest among those calculated. The relationship between the virtual packing density (γ_i) and the actual packing density (Φ) is given by the compaction index (K), calculated by Equation 4 [31]. The compaction index depends on the applied compaction energy. A 12.2 compaction index was determined experimentally by Fennis [24] for fine particles under wet conditions.

$$K = \sum_{i=1}^{n} \frac{\frac{y_i}{\beta_i}}{\frac{1}{\Phi} - \frac{1}{\gamma_i}} \quad (4)$$

The determination of the packing density of each size class (β_i) is required for using the CPM. It can be calculated by the voids ratio for the aggregates, as per Equation 5, where β is the packing density, VR is the aggregate voids ratio, p_b is the bulk density and γ is the specific gravity.

$$\beta = 1 - VR = 1 - \left(\frac{\gamma - p_b}{\gamma} \right) = \frac{p_b}{\gamma} \quad (5)$$

However, Equation 5 cannot be used for the packing density of fine powders such as Portland cement and SCMs, which require measurements to be performed in the presence of water and chemical admixtures. Wet methods are suitable for fine particles because particles smaller than 125μm can present agglomeration [23], as previously mentioned. The agglomeration of the grains decreases the packing density of the material, and there may be variations in the measurements depending on the compaction method used [24], [32]. According to [33], there is no consensus on the best method for determining the packing density, but the mixing energy method described by Marquardt [34] is among the recommended. The method is based on the condition of grain dispersion in the mixture, as illustrated in Figure 1.

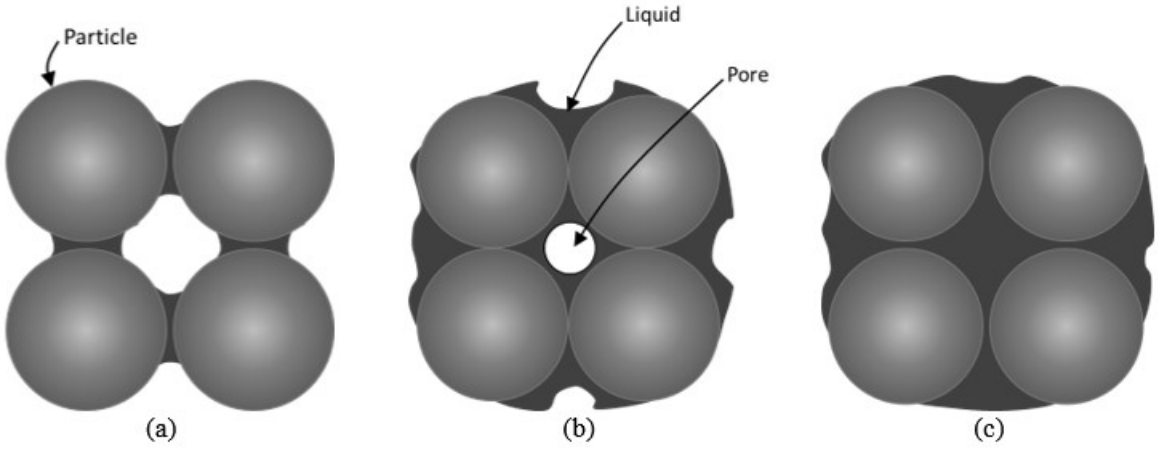

Figure 1 - Particle dispersion conditions in water: (a) pendulum bonds of water between the grains, (b) water film around all grains and (c) excess water pushes particles away from each other (adapted from Fennis [24]).

When slowly added, the water forms capillary bridges between the grains, called pendulum bonds. If it is added in small amounts, the water volume will not be enough to involve all the particles completely and will concentrate

at the contact points between the grains (Figure 1a), promoting a certain distance between them and, consequently, decreasing the solids concentration of the mixture. As the water to solids ratio (w/s) increases, the condition of continuity of the water film around all grains is reached, so that the particles move closer to each other due to the surface tension of the water until the point where there is just enough water to wrap all the particles, but still with air pores inside the mixture. At this point (Figure 1b), the voids ratio is minimum, and the solids concentration is maximum. With the progressive increase of the w/s ratio after this point, the solids concentration decreases again, as the excess water in the mixture causes the particles in the system to move away from each other, becoming dispersed in water (Figure 1c) [24], [35]–[37].

Marquardt [34] relates the water demand in each of the states described in Figure 1 with the energy consumption of the mixer during the pastes mixing process, with constant water addition. The test principle is based on the shearing forces at different humidity levels. A dry powder will show little shear strength, resulting in low energy consumption. By gradually adding water to the mix, the pendulum forces between the particles increase. With that, the shear strength and energy consumption of the mixing equipment also increase until they reach a maximum. By continuing the addition of water, the particles move apart, leading to liquefaction of the mixture and a decrease in the recorded energy [24], [38].

3 MATERIALS AND METHODS

3.1 Materials characterization

A Brazilian CPV-ARI Portland cement was used in this study, according to NBR 16697 [39]. The manufacturer provided its physical-chemical characterization while calcium carbonate and calcium hydroxide content were evaluated by thermogravimetry (Figure 2). The test was performed in anhydrous and hydrated samples measured in a Thermal Analysis System (labsys Evo DTA/DSC, Setaram Instrumentation), operating at 10ºC/min up to 1000ºC, under an argon atmosphere. A hydrated cement paste with 0.4 water/binder ratio was evaluated at 91 days. Hydration stoppage was performed by solvent exchange as per RILEM TC-238 SCM. The calcium hydroxide was calculated based on water loss between 400ºC and 600ºC [$Ca(OH)_2 = 4.11 \,.\, H_2O$] and calcium carbonate was calculated based on CO_2 release between 600 ºC and 1000ºC [$CaCO_3 = 2.27 \,.\, CO_2$] [40]–[44].

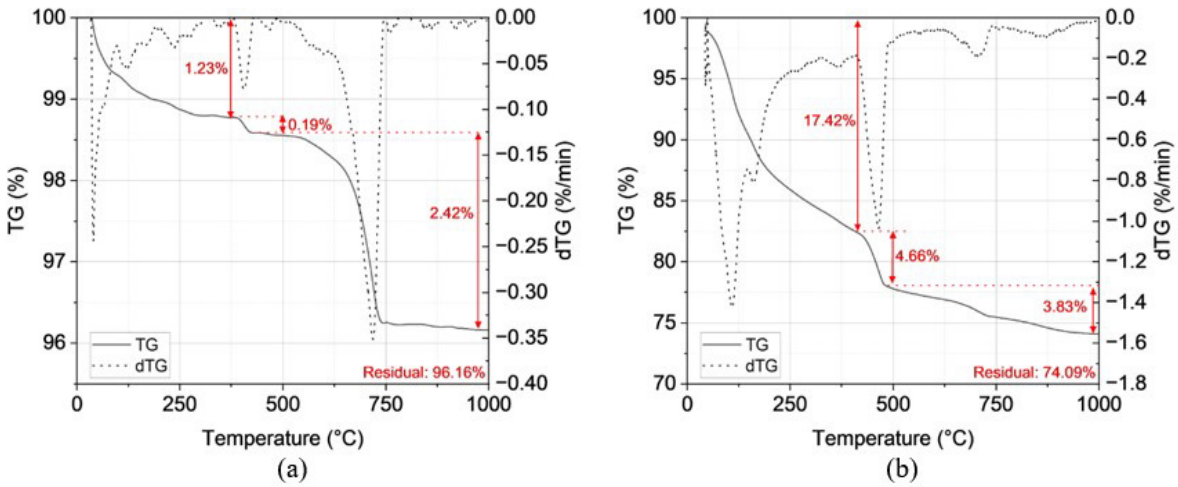

Figure 2 - Thermal analysis of (a) anhydrous Portland cement and (b) 91 days hydrated Portland cement paste

The 5.50% calcium carbonate content (5.71% in non-volatile base) associated with the limestone filler in the anhydrous Portland cement and the 19.16% calcium hydroxide content (25.86% in non-volatile base) related to the portlandite phase available after cement hydration were estimated by the test.

Limestone filler, fly ash, metakaolin and densified silica fume were used as SCMs. According to NBR 13956 [45], silica fume is considered densified when the material is subjected to beneficiation by agglomeration of the particles – being the most commercialized form for applications in cementitious materials [46]. The specific gravity of the SCMs was obtained by the authors as per NBR 16605 [47].

The particle size distribution of the cement and SCMs was obtained by laser diffraction in a particle size analyzer (CILAS 920), using 850 nm diode LASER. The dispersion of the materials was performed by pulverization in a 355 µm sieve, dissolution in water, and 60s of ultrasound coupled to the equipment [21], [48]. Due to the smaller average size of its particles, the silica fume's particle size distribution was evaluated by the Dynamic Light Scattering technique (Microtrac Nanotrac), which uses a 785 nm laser with reflection measurements. Sample dispersion was performed by dissolution at 2 mg/ml in distilled water with 5% superplasticizer chemical admixture (PowerFlow 4001, polycarboxylate base) in an ultrasonic bath (Schuster L-100, 160W, 42000 Hz) for 15 minutes. The particle size distribution of sand was performed by sieving according to NBR NM 248 [49] and can be seen in Figure 3.

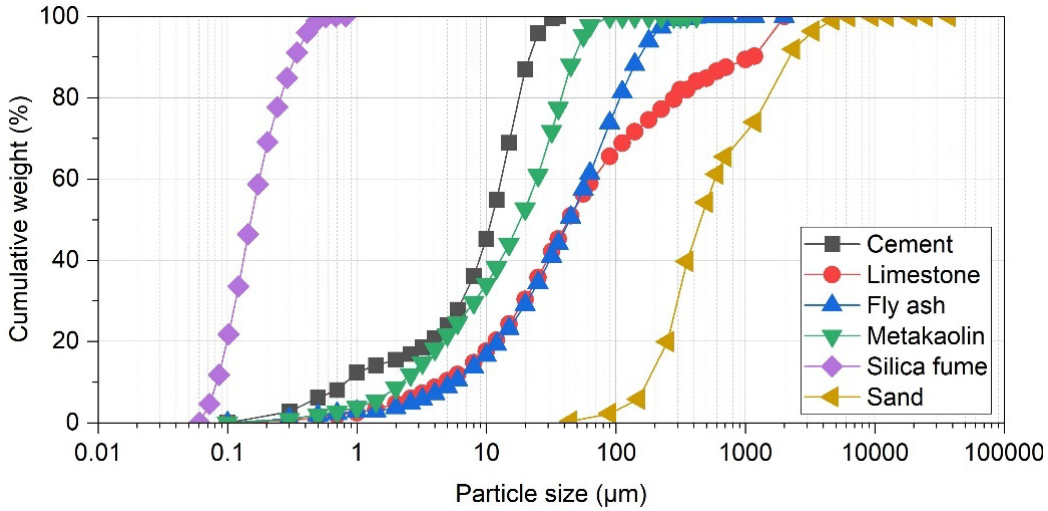

Figure 3 - Particle size distribution of the materials

The SCMs were characterized by X-ray fluorescence, fixed calcium hydroxide content (modified Chapelle test method) and specific gravity according to NBR 16605 [47]. The X-ray fluorescence (Rigaku ZSX Primus II) was performed after pulverizing the material on a 355 µm sieve and pressing it into tablet form, using boric acid as a binder. The results of the chemical analysis presented in Table 2 were duly corrected by loss on ignition at 950°C. The fixed calcium hydroxide content (Modified Chapelle) was performed according to NBR 15895 [50]. For the test, calcium oxide and SCMs are mixed in a 2:1 ratio by mass at 90°C for 16 hours in a solution with distilled water. After the determined period, the remaining (free) lime content is titrated with hydrochloric acid, using phenolphthalein as an indicator. It is worth mentioning that all SCMs presented results above 436 mg/g, stablished by Raverdy et al. [51] to classify pozzolanic materials, and the metakaolin presented a similar reactivity when compared to the densified silica fume. The mineralogical composition of the powdered materials (Figure 4) was carried out by X-ray diffraction (Rigaku, Ultima IV, operating at 40 kV/30mA, 5° to 75°, 0.02°step, 2°/min scan speed). The data interpretation was based on the 2021 COD crystallographic database.

Table 2 - Chemical characterization of the fine materials.

Material	Chemical composition (%)									Specific gravity (g/cm^3)	Modified Chapelle (mg/g)
	SiO_2	Al_2O_3	Fe_2O_3	CaO	SO_3	MgO	K_2O	Other	LOI		
Cement	19.08	4.38	2.97	61.57	3.08	3.15	0.00	2.19	3.58	3.130	-
Limestone filler	9.21	3.02	0.63	42.63	0.11	5.57	0.44	0.03	38.37	2.784	-
Fly ash	59.48	26.98	4.04	1.36	0.57	0.92	3.06	2.10	1.50	2.000	660.76
Metakaolin	50.41	42.99	1.68	0.08	0.04	0.20	1.41	1.47	1.71	2.492	1265.67
Silica fume	94.07	0.20	0.06	0.31	0.12	0.71	0.82	0.55	3.17	1.972	1276.76

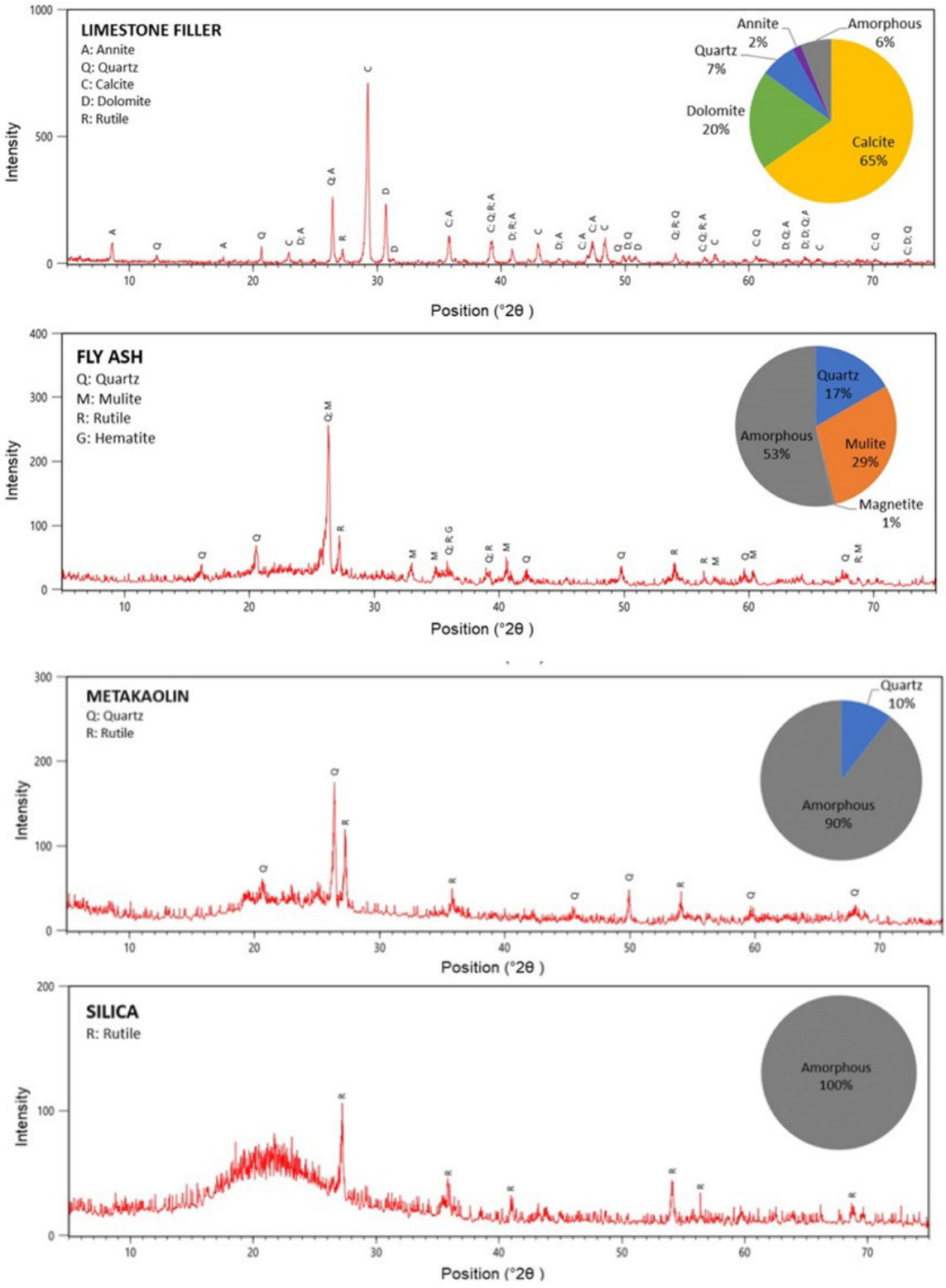

Figure 4 - Mineral composition of the SCMs

In this study, natural quartz was used as a fine aggregate. The aggregate was evaluated by specific gravity (2.70 g/cm^3) according to NBR 16916 [52], bulk density according to NBR 16972 (1.58 g/cm^3) [53], water absorption according to NBR 16916 [52] (1.40%), particle size distribution by sieving (457.89 µm average diameter) according to NM 248 [49], and packing density (β=0.586) according to Equation 5. A third-generation chemical admixture of modified carboxylic ether polymers (MC-Bauchemie, PowerFlow4001) with 1.12 g/cm^3 specific gravity was used. The saturation point of 1% by cement weight was determined by Kantro's method [54] in a 0.3 water to solids ratio for Portland cement paste. It was kept constant in all mixes, including the SCMs. Due to the small particle size, the SCMs may demand higher ratios of chemical admixtures, resulting in a mechanical behavior different from field [55].

The mixing energy method [56] evaluated the packing density and water demand of the fine materials. Higher energy consumption is expected when the funicular state is reached since the mixture will reach higher shear stress due to the proximity of the particles [24]. The test was performed in duplicate for the cement and SCMs, and the packing density (β) was calculated according to Equation 6, in which V_s is the volume of solid materials (cm^3); V_a is the volume of chemical admixture (cm^3) and; V_w is the volume of water, at the maximum energy consumption.

$$\beta = \frac{V_s}{V_s+V_a+V_w} \tag{6}$$

Adaptations on the initial volume of paste and water were made to perform the test on SCMs since it was developed for Portland cement. Table 3 shows the parameters used for each material. For the mixing, the initial water with superplasticizer admixture and all dry material is placed in the bowl, the mortar mixer is turned on at low speed for 60 seconds, followed by 60-second resting time. Then, the mixing is resumed at low speed with a constant addition of water of 1.5 ml/s with the aid of an intravenous dripper. The test is conducted until the mixture is liquefied (taking less than 250s). The energy consumption was monitored during the mixing process using an Arduino Nano with SCT013 current sensor. Based on these results, it was possible to calculate (Equation 6) the packing density and the water demand for the pastes, presented in Table 3 which also indicates the initial water to solids (w/s) ratio used in the test procedure.

Table 3 - Parameters used for the mixing energy test, the packing density and the water demand results obtained from the test.

Material	Initial dry mass (kg)	Initial w/s (by weight)	Packing density (-)	Minimum w/s, by volume (-)	Minimum w/s, by weight (-)
Portland cement	1.00	0.176	0.597	0.619	0.194
Fly Ash	1.00	0.088	0.704	0.402	0.200
Limestone filler	1.00	0.176	0.578	0.704	0.126
Metakaolin	1.00	0.264	0.455	1.177	0.472
Silica fume	0.75	0.606	0.344	1.885	0.677

Further details on the mixing energy method setup, investigation of the test parameters and power consumption for different SCMs can be verified at Soto et al. [56]. The results obtained for the cement and SCMs were used for the proportioning of the mortars studied by particle packing.

3.2 Mortars mix design

For the mortar mix design, four different compositions were developed: one containing sand, cement and limestone filler (which shall be referred to as PC composition); and three partially replacing Portland cement by fly ash (FA composition), metakaolin (MK composition) or silica fume (SF composition) – as per Table 4. Aiming for an eco-efficient material, the mixtures were developed considering the calcium hydroxide content available in the Portland cement after 91 days and the chemical combination capacity of the SCMs. The use of high levels of SCMs does not cause a significant decrease in the alkalinity of concrete, however, it can destabilize some hydrated phases [57]. The modified Chapelle test overestimates the reaction capacity of SCMs due to high temperature and excess of water. Thus, its use to establish the maximum replacement level of cement works towards safety since it does not deplete the portlandite content.

Lothenbach et al. [58] explain that it is essential that there is remaining portlandite after the initial pozzolanic activity (after 90 days) because the solubility of amorphous silica is sensitive to pH variations, and the higher the pH the higher the reaction rate. As long as enough OH^- ions remain in solution to maintain the pore solution's pH high, the active SCMs reactions will continue in the long term, at a very small rate. Additionally, by fixing the cement replacement ratio, it is possible to design mixtures using the CPM without excessive levels of SCMs, which could significantly reduce the composite strength [59]. Finally, fixing the Portland cement replacement ratio allows the optimization of limestone filler and sand for the packing density that helps decrease the CO_2 emission of the mortars.

Equation 7 calculates the maximum replacement level of cement by SCM ($\%\,SCM$), where $\%\,Ca(OH)_2$ is the available Portlandite content at 91 days and $Chapelle$ is the modified Chapelle test result (expressed as $gCa(OH)_2$/gSCM) [60], [61]. Therefore, considering the 19.16% of portlandite content in cement and the modified Chapelle test results, the maximum substitution rate ($\%\,SCM$) was calculated for the fly ash (22.47%), metakaolin (13.14%) and silica fume (13.05%).

$$\%\,SCM = \frac{\%\,Ca(OH)_2}{Chapelle + \%\,Ca(OH)_2} \tag{7}$$

Thus, the cement replacement level was fixed for each SCM based on Equation 7, while sand, limestone filler and binders (Portland cement + SCM, at a fixed proportion) varied to achieve the highest packing density using the CPM. The average dimension (d_i) and packing density (β_i) of each size class (it was considered that each fine material composed a grain size class, represented by its average size) were experimentally determined, as previously presented in section 3.1. Due to the high number of possible combinations to be calculated, it was used a ten-point simplex mixture design to simulate the packing density, plot a response surface (Figures 5, 6, 7 and 8) and find the optimum combination (desirability functions). Equations describing each response surface are shown in Equations 8 to 11, where the packing density (Φ) is expressed as a function of components percentage. These optimized combinations were then fed back to the CPM for error calculation.

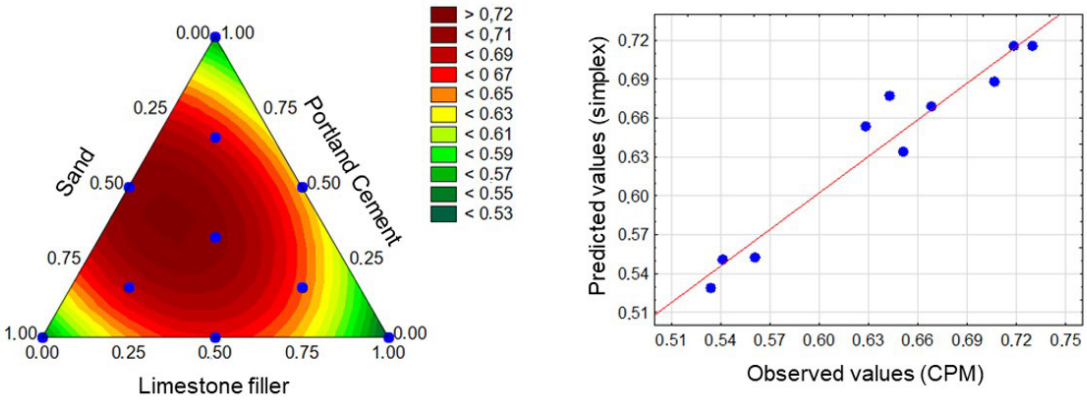

Figure 5 - Response surface for packing density of combinations of sand, Portland cement and filler for the PC composition.

$$\Phi = 0.5507.\%Sand + 0.5287.\%Limestone\ filler + 0.5525.\%Portland\ cement + 0.5161.\%Sand.\%Limestone\ filler + 0.6555.\%Sand.\%Portland\ cement + 0.3717.\%Limestone\ filler.\%Portland\ cement \tag{8}$$

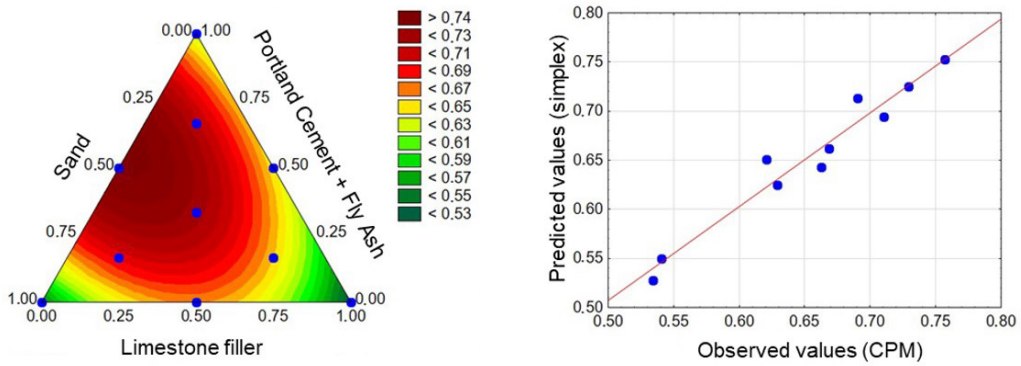

Figure 6 - Response surface for packing density of combinations of sand, Portland cement, fly ash and filler for the FA composition.

$$\Phi = 0.5507.\%Sand + 0.5278.\%Limestone\ filler + 0.6248.(\%Portland\ cement + \%Fly\ ash) + 0.4910.\%Sand.\%Limestone\ filler + 0.6614.\%Sand.(\%Portland\ cement + \%Fly\ ash) + 0.2676.\%Limestone\ filler.(\%Portland\ cement + \%Fly\ ash) \quad (9)$$

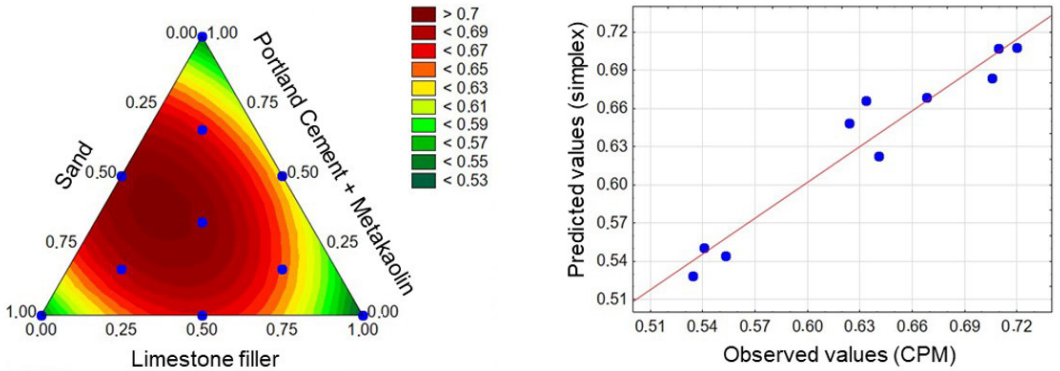

Figure 7 - Response surface for packing density of combinations of sand, Portland cement, metakaolin and filler for the MK composition.

$$\Phi = 0.5516.\%Sand + 0.5286.\%Limestone\ filler + 0.5444.(\%Portland\ cement + \%Metakaolin) + 0.5160.\%Sand.\%Limestone\ filler + 0.6366.\%Sand.(\%Portland\ cement + \%Metakaolin) + 0.3454.\%Limestone\ filler.(\%Portland\ cement + \%Metakaolin) \quad (10)$$

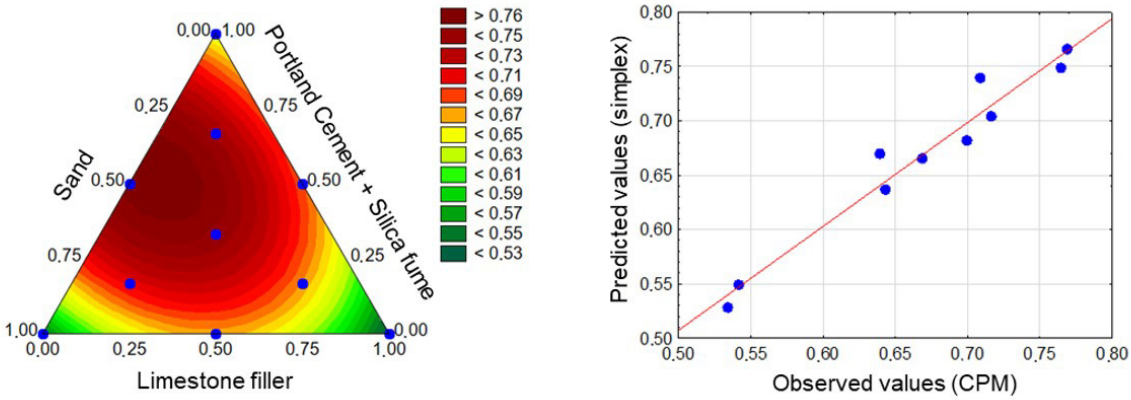

Figure 8 - Response surface for packing density of combinations of sand, Portland cement, silica fume and filler for the SF composition.

$$\Phi = 0.5491.\%Sand + 0.5278.\%Limestone\ filler + 0.6365.(\%Portland\ cement + \%Silica\ fume) + 0.5057.\%Sand.\%Limestone\ filler + 0.6904.\%Sand.(\%Portland\ cement + \%Silica\ fume) + 0.3982.\%Limestone\ filler.(\%Portland\ cement + \%Silica\ fume) \quad (11)$$

Based on the quadratic model, it was possible to determine the combination of factors (sand, limestone filler and binder) to obtain the highest actual packing density using a desirability function. The optimal combination obtained from the response surface analysis was then applied to the CPM model for validation and error calculation – Table 4. It can be noticed that the fly ash composition (FA) does not contain limestone filler in its formulation. This occurs because the fly ash and the limestone filler present very similar average sizes and, in the analysis of the possible variations of this composition, any addition of filler entailed a decrease in packing density. After establishing the optimal mixture design by the CPM, the mixing energy test was again performed on the mortars to determine the water demand (Table 4), therefore, establishing water to binder ratio. The mortars mixing and casting procedure followed NBR 13279 [62], and the prismatic samples (40x40x160) mm were cured by immersion in lime-saturated water as per NBR 9479 [63] to avoid leaching.

Table 4 - Mix design of mortars optimized by the Compressible Packing Model.

Composition	Sand	Cement	Limestone filler	Fly ash	Metakaolin	Silica Fume	Packing density	Model error	w/b ratios (by weight)
PC Portland cement	43.20%	39.69%	17.11%	-	-	-	0.7355	1.64%	0.207
FA Fly ash	44.42%	43.09%	0.00%	12.49%	-	-	0.7428	-1.67%	0.211
MK Metakaolin	43.95%	33.00%	18.05%	-	5.00%	-	0.7314	2.15%	0.218
SF Silica Fume	40.99%	45.79%	6.35%	-	-	6.87%	0.7582	-1.46%	0.226

Since the strength is directly associated to the gel-space ratio due to the formation of capillary pores, as established by Brouwers [64], the increase in water to binders ratio will proportionally reduce the strength for all mortars; while water to binders ratio ratios lower than the water demand will generate defects and high-stress concentration around the flaw resulting in the fracture of material also reducing the strength, according to Griffith' Theory [65].

3.3 Mortar characterization

In the fresh state, a semi-adiabatic calorimetry (SM-125 optical interrogator using a 1550 nm FBG sensor) was performed on the mortars considering RILEM TC 119-TCE recommendations. The setting time was established by the derivate technique [66]. In the hardened state, samples were submitted to flexural and axial compressive strength tests as per NBR 13279 [62]. The mortar samples were also submitted to thermogravimetric analysis at 91 days (TG-RB3000, BP Engenharia, operating at 10ºC/min up to 1000ºC with 10g sample) to evaluate the chemical composition and portlandite consumption due to the SCMs substitution - the calculated values were corrected for a non-volatile base so the results could be compared among them [67]. Finally, the binder index expressed as a relationship between the cement consumption (kg/m^3) and the compressive strength (MPa), and CO_2 emission of the compositions were calculated based on values presented in Table 1.

4 RESULTS AND DISCUSSION

In the fresh state, the mortars were evaluated by semi-adiabatic calorimetry (Figure 9). All mortars presented an induction period related to the step-retreat dissolution mechanism until the supersaturation of the solution with intense precipitation of C-S-H over C_3S. With a calcium supersaturated solution, there is an increase in temperature for all mortars due to the simultaneous precipitation of portlandite and high Ca/Si ratio C-S-H [67]. Since all mortars with SCMs presented an increase in temperature and reduction in the setting time when compared to the mortar containing only Portland cement (PC), it is possible to establish that highly reactive SCMs can also interfere with the dissolution and precipitation process due to its chemical properties and amorphous content – even when presenting coarser particles that would reduce the nucleation effect. After the temperature peak, it was not possible to observe any defined thermal event.

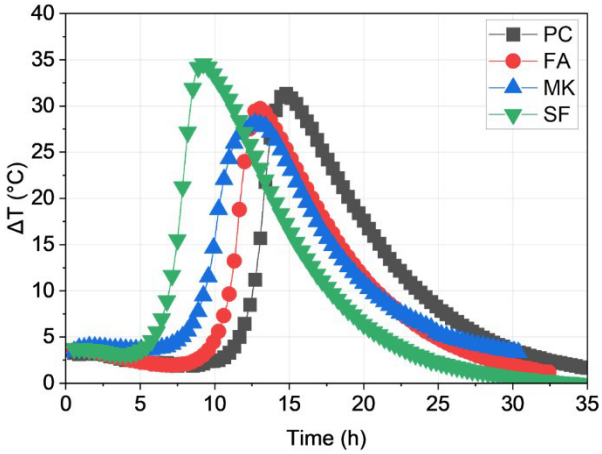

Figure 9 - Semi-adiabatic calorimetry of the mortars containing Portland cement (PC), fly ash (FA), metakaolin (MK) and silica fume (SF).

In the hardened state, samples were submitted to mechanical tests at 28 and 91 days (Figure 10). Based on the Tukey means comparison test (α=0.05), only mortar samples containing fly ash (FA) and metakaolin (MK) presented a statistically significant increase in strength from 28 to 91 days caused by latent pozzolanic reactions. The PC composition did not increase strength from 28 to 91 days due to the high early strength cement used. FA mortar had a higher content of SCM (12.49% of fly ash) and Portland cement (44.42% of Portland cement), explaining its higher compressive strength at 91 days. Due to the absence of limestone filler in FA composition, the formation of hydrated phases such as C-S-H was optimized. Mortars with silica fume (SF) reached maximum strength at 28 days, which is explained by the accelerated reaction due to its fine particles (nucleation effect), its low amount on the mixture (6.87%) and high amorphous content (Figure 4). Particles finer than cement can promote heterogeneous nucleation of hydrates on foreign mineral particles, which catalyzes the nucleation process by reducing the energy barrier [68]; while a high amorphous content of the silica fume promotes a rapid dissolution and reaction with portlandite to precipitate C-S-H [69], hence, increasing the SF composition strength.

Additionally, fly ash mortar reached the highest compressive strength of 118 MPa at 91 days. Based on Figure 10, a proportional linear relationship between flexural and compressive strength of 18.95% can be calculated for the samples. A proportion around 20% is expected for cementitious materials [70]. Reinhardt [71] explain that high strength composites containing SCMs have a densified interfacial transition zone, and the absence of coarse aggregates reduces the mesoscale defects. This difference has an important effect on cracking development and is also responsible for a higher tensile strength of the mortars compared to conventional mortars and concretes.

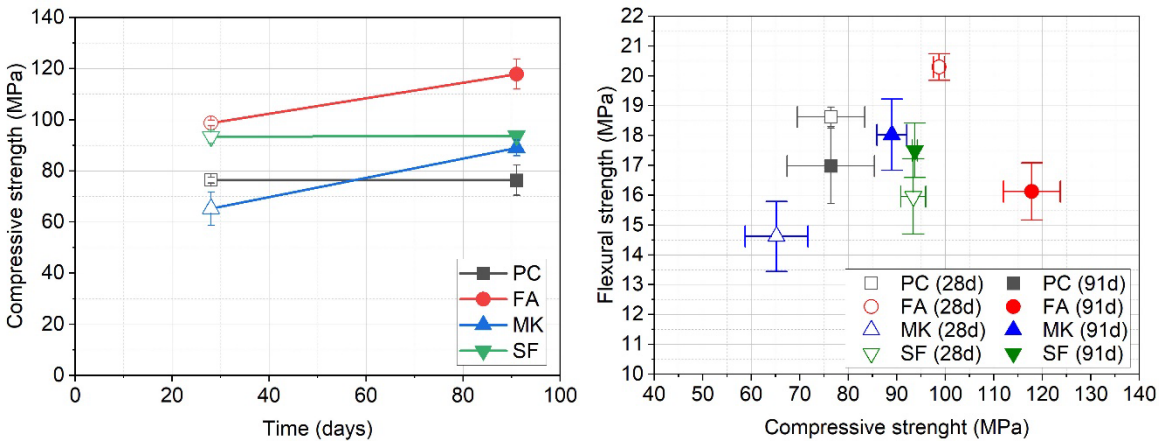

Figure 10 – (a) Compressive strength and (b) correlation between compressive and flexural strengths of mortars containing Portland cement (PC), fly ash (FA), metakaolin (MK) and silica fume (SF)

Some correlations between compressive strength and water to cement (w/c) ratios are shown in Figure 11. According to Bentz and Aitcin [72], the w/c ratio can be directly related to the spacing between the cement particles in the paste. The smaller the w/c ratio, the smaller this spacing, and the faster the hydrated phases will fill the voids (reducing porosity) and creating stronger bonds that result in a higher mechanical strength. Although the SCMs can help to improve the packing density (filler effect) and generate additional C-S-H phases (pozzolanic reactions), the pore refinement happens on a micro-scale that has a lower impact on the mechanical strength than the w/c ratio. Therefore, as can be seen in Figure 11, higher strengths are reached when mortars have lower water demand, hence, lower w/c ratios. This way, even with higher cement content and reactivity of the MK and SF compositions, the FA composition performed better due to the lower w/c ratio.

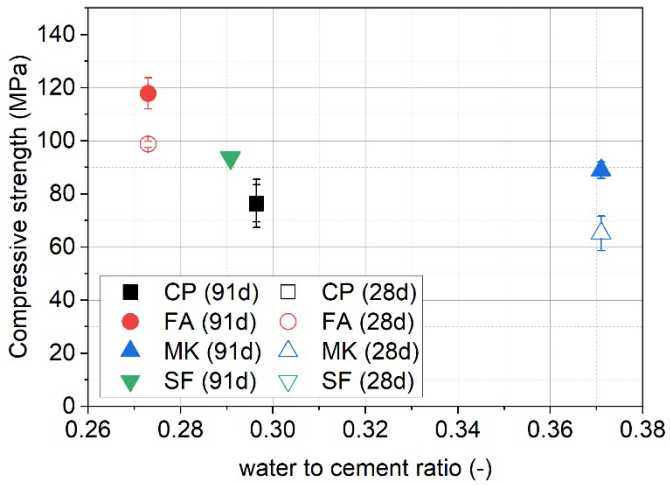

Figure 11 - Correlation between the compressive strength and the w/c ratio

Based on thermogravimetric analysis in Figure 12, it was possible to calculate the chemically bounded water (CBW) from C-S-H and aluminates, portlandite [$Ca(OH)_2 = 4.11\,.H_2O$] and calcite [$CaCO_3 = 2.27\,.CO_2$] content after 91 days. The mortar sample with Portland cement (PC) presented the lowest content in hydrates, reinforcing the additional hydrated phases formed due to the use of SCMs in the other compositions, with an increase in the chemically bounded water (CBW) (Figure 13).

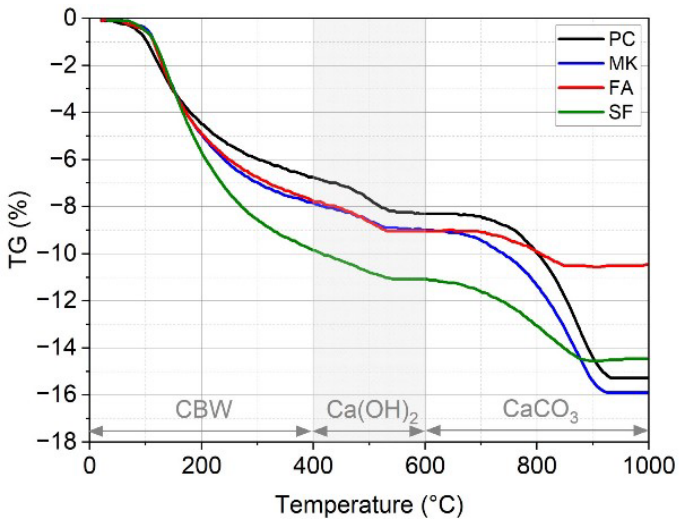

Figure 12 - Mass loss of mortars during thermogravimetry test.

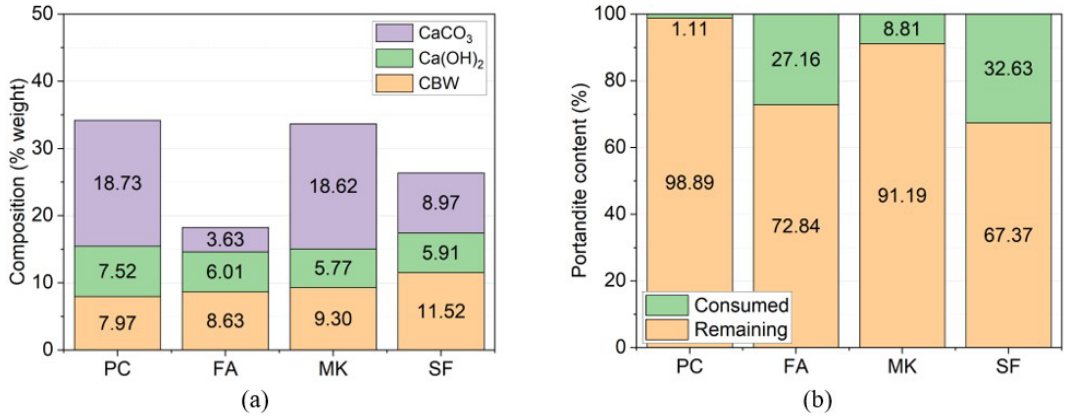

Figure 13 –Mortars (a) chemical composition (nonvolatile base) and (b) Portlandite consumption after 91 days.

Although the modified Chapelle test was used to establish the Portland cement substitution, the total depletion of portlandite did not happen. This behavior is explained by the different conditions of the mortar mixing and the test mixing procedure (solution at 90°C), as previously discussed. The consumed portlandite content was calculated considering the difference between the initial and final content of the mineral phase. The initial content was calculated from the mortar theoretical compositions and Portland cement portlandite quantification by TG (Figure 2b), while the remaining base content was established based on the mortars TG (Figure 13a). Results presented in Figure 13b were normalized to allow comparison among samples. PC presented a 1% variation, related to TG quantification errors, since no SCM was used in this composition and there was not any additional $Ca(OH)_2$ consumption due to the pozzolanic reaction. FA and SF showed a higher consumption of portlandite and higher strength values. This behavior can be related to the higher portlandite content in the FA mortars (absence of limestone filler) and the high reactivity of the silica fume (100% amorphous) in the SF mortars. Despite high reactivity, the metakaolin (MK) consumed only 8% of the available base. Notice that FA and SF were added in compositions with approximately 43% and 46% of Portland cement, respectively (Table 4). Meanwhile only 5% of metakaolin in a 33% Portland cement composition (MK mortar) slowed the portlandite consumption. This behavior highlights the importance of an alkaline content in the hydration kinetics due to its influence on the solubility of amorphous silica for the formation of C-S-H. Regarding the calcite content, the mass loss was proportional to the limestone filler content in the samples. The 3% present in FA composition is related to the limestone filler in Portland cement, since no extra limestone filler was used.

Finally, the mortars were evaluated in terms of sustainability. Figure 14(a) shows the consumption of cement per unit of compressive strength for each analyzed age, a parameter known as the binder index. Figure 14(b) presents the produced mortars' total CO_2 emissions per MPa.

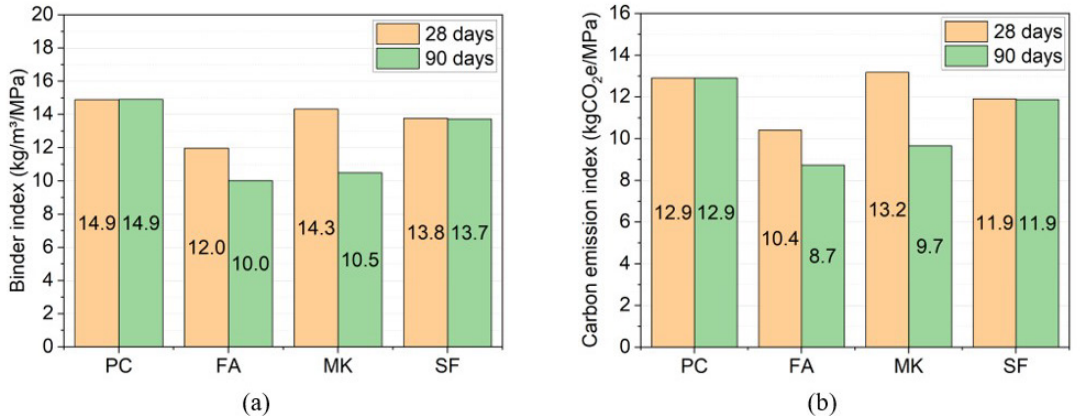

Figure 14 – (a) Cement consumption required to obtain 1 MPa of compressive strength and (b) CO2e emission of mortars containing Portland cement (PC), fly ash (FA), metakaolin (MK) and silica fume (SF).

The mixture with fly ash (FA) obtained the lowest binder index, of 10.0 kg/m^3/MPa. This composition was the most efficient mixture, with the highest compressive strength at 91 days [73]. developed a study to produce mortars that incorporate SCM suitable to two-stage concrete and achieved binder index values between 10.3 and 17.3 kg/m^3/MPa [74]. also developed a study to produce mortars and achieved values between 14.4 and 19 kg/m^3/MPa for mortars incorporating polymer powder. So, the results presented in this work highlighted the efficiency of the mortars produced by the proposed method.

The mortar containing fly ash (FA) also presented the lowest carbon emission index at 91 days, with an 8.73 kg CO_2e/MPa emission. The composition had up to 30% reduction in CO_2e/MPa emissions compared to the mortar with only Portland cement (PC) [5]. estimated the average CO_2e/MPa ratio found in the literature is 7.1 for concretes produced worldwide and 9.1 for Brazilian concretes. Therefore, this study achieved similar CO_2e/MPa ratios in high-strength mortars, and these values may still be reduced as coarse aggregates were not used in this study [75]. also evaluated the CO_2e emissions of pastes, achieving values between 7.5 and 9.9 kg CO_2e/MPa. These results indicate that the mix design proposed in this study can be used to obtain eco-efficient mortars in terms of cement consumption and CO_2 emissions.

5 CONCLUSIONS

The study demonstrated that the reactivity of the SCMs (based on the modified Chapelle test) can be used to establish the Portland cement substitution. The mixing energy method successfully allowed the estimation of the raw materials' packing density and the mortars' water demand. Those approaches simplified the use of the CPM model, prevented the presence of unreacted SCMs in the mixtures and optimized the use of limestone filler and sand, which have a lower environmental impact. The association of the simplex mixture design with the CPM model reduced the iterations required to calculate the packing density and facilitated the definition of the optimal mixture design with a low error.

The evaluated mortars reached 118MPa of compressive strength at 91 days, with binder indexes between 10 and 15 kg/m^3/MPa and up to 30% reduction in CO_2e/MPa emissions. Those results emphasize the low environmental impact of those mixtures and how particle packing theory, specifically the CPM, can aid the development of high-strength eco-friendly composites.

ACKNOWLEDGEMENTS

The authors would like to thank the companies Itambe, Pozofly, Metacaulim do Brasil, MC-Bauchemie and Tecnosil, which kindly provided all the necessary materials. We also extend our thanks to the CESEC (Center for Civil Engineering Studies) and LAME (Laboratory of Materials and Structures) at the Federal University of Parana, UFPR, for their infrastructure. Additionally, we appreciate the support from the Post-graduated Program in Civil Engineering (PPGEC/UFPR), the Multi-User Photonics Facility at Federal University of Technology – Parana (UTFPR), and the C-LABMU Multi-User Complex at State University of Ponta Grossa (UEPG).

REFERENCES

[1] J. M. F. Carvalho, T. V. D. Melo, W. C. Fontes, J. O. D. S. Batista, G. J. Brigolini, and R. A. F. Peixoto, “More eco-efficient concrete: An approach on optimization in the production and use of waste-based supplementary cementing materials,” *Constr. Build. Mater.*, vol. 206, pp. 397–409, 2019, http://dx.doi.org/10.1016/j.conbuildmat.2019.02.054.

[2] U.S. Geological Survey, *Mineral commodity summaries 2020*. U.S.: Geological Survey, 2020.

[3] P. R. Matos, R. D. Sakata, and L. R. Prudêncio, “Eco-efficient low binder high-performance self-compacting concretes,” *Constr. Build. Mater.*, vol. 225, pp. 941–955, 2019, http://dx.doi.org/10.1016/j.conbuildmat.2019.07.254.

[4] V. Masson-Delmotte et al., *Global Warming of 1.5°C: an IPCC Special Report on the impacts of global warming of 1.5°C above pre-industrial levels and related global greenhouse gas emission pathways, in the context of strengthening the global response to the threat of climate change*. Geneva: World Meteorological Organization, 2019.

[5] B. L. Damineli, F. M. Kemeid, P. S. Aguiar, and V. M. John, “Measuring the eco-efficiency of cement use,” *Cement Concr. Compos.*, vol. 32, pp. 555–562, 2010, http://dx.doi.org/10.1016/j.cemconcomp.2010.07.009.

[6] International Energy Agency, *Technology Roadmap - Low-Carbon Transition in the Cement Industry*. Paris: IEA, 2018.

[7] S. A. Miller, P. J. M. Monteiro, C. P. Ostertag, and A. Horvath, “Comparison indices for design and proportioning of concrete mixtures taking environmental impacts into account,” *Cement Concr. Compos.*, vol. 68, pp. 131–143, 2016., http://dx.doi.org/10.1016/j.cemconcomp.2016.02.002.

[8] J. Hoppe Fo, A. Gobbi, E. Pereira, V. A. Quarcioni, and M. H. F. Medeiros, Atividade pozolânica de adições minerais para cimento portland (Parte i): índice de atividade pozolânica (IAP) com cal, difração de raios-x (DRX), termogravimetria (TG/DTG) e chapelle modificado, *Revista Materia*, vol. 22, pp. e11872, 2017. https://doi.org/10.1590/S1517-707620170003.0206.

[9] A. Nazari and J. G. Sanjayan, *Handbook of low carbon concrete*. Oxford: Butterworth-Heinemann, 2016.

[10] S. A. Miller, "Supplementary cementitious materials to mitigate greenhouse gas emissions from concrete: can there be too much of a good thing," *J. Clean. Prod.*, vol. 178, pp. 587–598, 2018., http://dx.doi.org/10.1016/j.jclepro.2018.01.008.

[11] K. L. Scrivener, V. M. John, and E. M. Gartner, "Eco-efficient cements: potential economically viable solutions for a low-CO2 cement-based materials industry," *Cement Concr. Res.*, vol. 114, pp. 2–26, 2018, http://dx.doi.org/10.1016/j.cemconres.2018.03.015.

[12] M. V. Shoubi, A. S. Barough, and O. Amirsoleimani, "Assessment of the roles of various cement replacements in achieving the sustainable and high performance concrete," *Int. J. Adv. Eng. Technol.*, vol. 6, pp. 68–77, 2013.

[13] Sindicato Nacional da Indústria do Cimento, *Roadmap tecnológico do cimento: potencial de redução das emissões de carbono da indústria do cimento brasileira até 2050*. Rio de Janeiro: SNIC, 2019.

[14] B. Pacewska and I. Wilińska, "Usage of supplementary cementitious materials: advantages and limitations," *J. Therm. Anal. Calorim.*, vol. 142, pp. 371–393, 2020., http://dx.doi.org/10.1007/s10973-020-09907-1.

[15] K. L. Scrivener et al., "TC 238-SCM: hydration and microstructure of concrete with SCMs: state of the art on methods to determine degree of reaction of SCMs," *Mater. Struct.*, vol. 48, pp. 835–862, 2015. https://doi.org/10.1617/s11527-015-0527-4

[16] M.J. Tapas, "Role of supplementary cementitious materials in mitigating alkali-silica reaction," Doctoral dissertation, University of Technology Sydney, Sydney, Australia, 2020.

[17] S. Yousuf, L. F. M. Sanchez, and S. A. Shammeh, "The use of particle packing models (PPMs) to design structural low cement concrete as an alternative for construction industry," *J. Build. Eng.*, vol. 25, pp. 100815, 2019., http://dx.doi.org/10.1016/j.jobe.2019.100815.

[18] C. Londero, N. S. Klein, and W. Mazer, "Study of low-cement concrete mix-design through particle packing techniques," *J. Build. Eng.*, vol. 42, pp. 103071, 2021., http://dx.doi.org/10.1016/j.jobe.2021.103071.

[19] H. F. Campos, N. S. Klein, and J. Marques Fo., "Proposed mix design method for sustainable high-strength concrete using particle packing optimization," *J. Clean. Prod.*, vol. 265, pp. 121907, 2020., http://dx.doi.org/10.1016/j.jclepro.2020.121907.

[20] A. L. De Castro and V. C. Pandolfelli, "Review: concepts of particle dispersion and packing for special concretes production," *Ceramica*, vol. 55, pp. 18–32, 2009., http://dx.doi.org/10.1590/S0366-69132009000100003.

[21] B. L. Damineli, R. G. Pileggi, and V. M. John, "Influence of packing and dispersion of particles on the cement content of concretes," *Rev. IBRACON Estrut. Mater.*, vol. 10, pp. 998–1024, 2017., http://dx.doi.org/10.1590/s1983-41952017000500004.

[22] I. Oliveira, A. Studart, R. Pileggi, and V. Pandolfelli, "Dispersão e empacotamento de partículas: princípios e aplicações em processamento cerâmico," *Fazendo Arte Ed.*, vol. 224, pp. 119–137, 2000.

[23] S. A. A. M. Fennis, J. C. Walraven, and J. A. Den Uijl, "Compaction-interaction packing mode: regarding the effect of fillers in concrete mixture design," *Mater. Struct.*, vol. 46, pp. 463–478, 2013. https://doi.org/10.1617/s11527-012-9910-6

[24] S.A.A.M. Fennis, "Design of ecological concrete by particle packing optimization" Doctoral dissertation, Technical University of Delft, Delft, Netherlands, 2011.

[25] S. A. A. M. Fennis, J. C. Walraven, and J. A. den Uijl, "Defined-performance design of ecological concrete," *Mater. Struct.*, vol. 46, pp. 639–650, 2013. https://doi.org/10.1617/s11527-012-9922-2

[26] D. R. Dinger, *Particle calculations for ceramists*. Kearney: Morris Pub, 2001.

[27] C. C. Furnas, "Grading Aggregates - I. mathematical relations for beds of broken solids of maximum density," *Ind. Eng. Chem.*, vol. 23, pp. 1052–1058, 1931., http://dx.doi.org/10.1021/ie50261a017.

[28] P. Goltermann, V. Johansen, and L. Palbøl, "Packing of aggregates: an alternative tool to determine the optimal aggregate mix," *Mater. J.*, vol. 94, pp. 435–443, 1997.

[29] J. Dewar, *Computer modelling of concrete mixtures*. London: CRC Press, 1999. https://doi.org/10.4324/9780203031148.

[30] T. Stovall, F. De Larrard, and M. Buil, "Linear packing density model of grain mixtures," *Powder Technol.*, vol. 48, pp. 1–12, 1986., http://dx.doi.org/10.1016/0032-5910(86)80058-4.

[31] F. De Larrard, *Concrete mixture proportioning*. London: CRC Press, 1999. https://doi.org/10.1201/9781482272055.

[32] P. Ballieu, "Design of ecological concrete by particle packing optimization" Masters dissertation, Universiteit Gent, Gent, Belgium, 2014.

[33] S. A. A. M. Fennis, "Measuring water demand or packing density of micro powders: comparison of methods," in *Design of ecological concrete by particle packing optimization*, Delft University, Netherlands, 2008, pp. 21. (Research paper)

[34] I. Marquardt, "Ein Mischungskonzept für selbstverdichtenden Beton auf der Basis der Volumenkenngrößen und Wasseransprüche der Ausgangsstoffe" Doctoral dissertation, Universitär Rostock, Rostok, German, 2001.

[35] H. F. Campos, T. M. S. Rocha, G. C. Reus, N. S. Klein, and J. Marques Filho, "Determination of the optimal replacement content of Portland cement by stone powder using particle packing methods and analysis of the influence of the excess water on the consistency of pastes," *Rev. IBRACON Estrut. Mater.*, vol. 12, pp. 210–232, 2019., http://dx.doi.org/10.1590/s1983-41952019000200002.

[36] N.S. Klein, "El rol físico del agua en mezclas de cemento portland". Doctoral dissertation, Universitat Politècnica de Catalunya, Barcelona, Espanha, 2012.

[37] L. G. Li and A. K. H. Kwan, "Concrete mix design based on water film thickness and paste film thickness," *Cement Concr. Compos.*, vol. 39, pp. 33–42, 2013., http://dx.doi.org/10.1016/j.cemconcomp.2013.03.021.

[38] M. Hunger, "An integral design concept for ecological self-compacting concrete" (Doctoral dissertation), Technische Universiteit Eindhoven, Eindhoven, Netherlands, 2010. https://doi.org/10.6100/IR674188.

[39] Associação Brasileira de Normas Técnicas, *Cimento Portland – Requisitos,* NBR 16697, 2018.

[40] M. Földvári, *Handbook of thermogravimetric system of minerals and its use in geological practice*. Budapest: Geological Institute of Hungary, 2011.

[41] J. Hoppe Fo., "Sistemas cimento, cinza volante e cal hidratada: mecanismo de hidratação, microestrutura e carbonatação de concreto" (Doctoral dissertation), Universidade de São Paulo, São Paulo, Brasil, 2008. https://doi.org/10.11606/T.3.2008.tde-19082008-172648.

[42] G. Niques, *"Efeito do tempo de maturação na microestrutura de uma cal virgem dolomítica"*, Masters dissertation, Universidade Federal de Santa Catarina, Florianópolis, Brasil, 2003.

[43] V. S. Ramachandran, R. M. Paroli, J. J. Beaudoin, and A. H. Delgado, *Handbook of thermal analysis of construction materials*. Sawston: Woodhead Publishing, 2002.

[44] W. W. Wendlandt, "Inorganic thermogravimetric analysis by Clement Duval," *Inorg. Chem.*, vol. 4, pp. 435–436, 1965., http://dx.doi.org/10.1021/ic50025a050.

[45] Associação Brasileira de Normas Técnicas, *Sílica ativa para uso com cimento Portland em concreto, argamassa e pasta Parte 1: Requisitos,* NBR 13956-1, 2012.

[46] N. T. A. Soto, G. Macioski, J. Hoppe Fo., and N. S. Klein "Caracterização físico-química da sílica ativa para aplicação como material cimentício suplementar", in: *Congresso Internacional de Construção Civil*, 2022, pp. 358–366.

[47] Associação Brasileira de Normas Técnicas, *Cimento Portland e outros materiais em pó — Determinação da massa específica,* NBR 16605, 2017.

[48] W. F. De Almeida, C. Matinc, A. B. Mendes, and O. Konrad, "Efeitos do uso de frequência de ultrassom na dispersão de sedimentos agregados," *Rev. Ibero-Americana Cienc. Ambientais.*, vol. 8, pp. 97–111, 2017., http://dx.doi.org/10.6008/SPC2179-6858.2017.003.0010.

[49] Associação Brasileira de Normas Técnicas, *Agregados - Determinação da composição granulométrica,* NBR NM 248, 2003.

[50] Associação Brasileira de Normas Técnicas, *Materiais pozolânicos - Determinação do teor de hidróxido de cálcio fixado - Método Chapelle modificado,* NBR 15895, 2010.

[51] M. Raverdy, F. Brivot, A. M. Paillere, and R. Dron, Appréciation de l'activité pouzzolanique de constituents secondaires, in: *Proceedings of the 7th International Congress on the Chemistry of Cement*, 1980, pp. 36–41.

[52] Associação Brasileira de Normas Técnicas, *Agregado miúdo - Determinação da densidade e da absorção de água,* NBR 16916, 2021.

[53] Associação Brasileira de Normas Técnicas, *Agregados - Determinação da massa unitária e do índice de vazios,* NBR 16972, 2021.

[54] P. Wedding and D. D. L. Kantro, "Influence of water-reducing admixtures on properties of cement paste: a miniature slump test," *Cem. Concr. Aggreg.*, vol. 2, pp. 95, 1980, http://dx.doi.org/10.1520/CCA10190J.

[55] J. Cheung, A. Jeknavorian, L. Roberts, and D. Silva, "Impact of admixtures on the hydration kinetics of Portland cement," *Cement Concr. Res.*, vol. 41, pp. 1289–1309, 2011, http://dx.doi.org/10.1016/j.cemconres.2011.03.005.

[56] N. T. A. Soto, G. Macioski, E. C. Araújo, J. Hoppe Fo., and N. S. Klein, Measuring packing density and water demand of Portland cement and SCMs by the mixing energy method, *Rev. IBRACON Estrut. Mater.*, vol. 16, no. 5, pp. e16507, 2023, http://dx.doi.org/10.1590/s1983-41952023000500007.

[57] B. Lothenbach and E. Wieland, *Chemical evolution of cementitious materials*. Brussels: NEA/RWM/R(2012)3/REV, 2012.

[58] B. Lothenbach, K. L. Scrivener, and R. D. Hooton, "Supplementary cementitious materials," *Cement Concr. Res.*, vol. 41, pp. 1244–1256, 2011., http://dx.doi.org/10.1016/j.cemconres.2010.12.001.

[59] M. Cyr, P. Lawrence, and E. Ringot, "Efficiency of mineral admixtures in mortars: quantification of the physical and chemical effects of fine admixtures in relation with compressive strength," *Cement Concr. Res.*, vol. 36, pp. 264–277, 2006, http://dx.doi.org/10.1016/j.cemconres.2005.07.001.

[60] H. F. Campos, N. S. Klein, and J. Marques Fo., "Comparison of the silica fume content for high-strength concrete production: chemical analysis of the pozzolanic reaction and physical behavior by particle packing," *Mater. Res.*, vol. 23, no. 5, pp. e20200285, 2020., http://dx.doi.org/10.1590/1980-5373-mr-2020-0285.

[61] G. Macioski, F. Perreto, N. T. A. Soto, and W. Mazer, "Estudo teórico da adição máxima de sílica ativa no ocimento Portland em função do consumo de hidróxido de cálcio," in: *XXI Congresso Brasileiro de Engenharia Química*, 2016, pp. 1–10.

[62] Associação Brasileira de Normas Técnicas, *Argamassa para assentamento e revestimento de paredes e tetos - Determinação da resistência à tração na flexão e à compressão* – NBR 13279, 2005.

[63] Associação Brasileira de Normas Técnicas, *Argamassa e concreto - Câmaras úmidas e tanques para cura de corpos-de-prova* – NBR 9479, 2006.

[64] H. J. H. Brouwers, "The work of powers and brownyard revisited: Part 1," *Cement Concr. Res.*, vol. 34, pp. 1697–1716, 2004, http://dx.doi.org/10.1016/j.cemconres.2004.05.031.

[65] T. Takahashi, M. Yamamoto, K. Ioku, and S. Goto, "Relationship between compressive strength and pore structure of hardened cement pastes," *Adv. Cement Res.*, vol. 9, pp. 25–30, 1997, http://dx.doi.org/10.1680/adcr.1997.9.33.25.

[66] X. Kang, H. Lei, and Z. Xia, "A comparative study of modified fall cone method and semi-adiabatic calorimetry for measurement of setting time of cement based materials," *Constr. Build. Mater.*, vol. 248, pp. 118634, 2020., http://dx.doi.org/10.1016/j.conbuildmat.2020.118634.

[67] K. Scrivener, R. Snellings, and B. Lothenbac, *A practical guide to microstructural analysis of cementitious materials*. Boca Raton: CRC Press, 2016.

[68] P. Lawrence, M. Cyr, and E. Ringot, "Mineral admixtures in mortars: effect of inert materials on short-term hydration," *Cement Concr. Res.*, vol. 33, pp. 1939–1947, 2003, http://dx.doi.org/10.1016/S0008-8846(03)00183-2.

[69] H. F. W. Taylor, *Cement Chemistry*. London: T. Telford, 1998.

[70] G. Mohamad, A. B. S. S. Neto, F. Pelisser, P. B. Lourenço, and H. R. Roman, "Caracterização mecânica das argamassas de assentamento para alvenaria estrutural - previsão e modo de ruptura," *Materia (Rio J.)*, vol. 14, pp. 824–844, 2009, http://dx.doi.org/10.1590/S1517-70762009000200006.

[71] H. W. Reinhardt, Factors affecting the tensile properties of concrete, in: J. Weerheijm, Ed. *Understanding the tensile properties of concrete*, United Kingdom: Elsevier, 2013, pp. 19–51. https://doi.org/10.1533/9780857097538.1.19.

[72] D. P. Bentz and P. C. Aitcin, "The hidden meaning of water-cement ratio," *Concr. Int.*, vol. 30, no. 5, pp. 51–54, 2008.

[73] M. F. Najjar, A. M. Soliman, and M. L. Nehdi, "Grouts incorporating supplementary cementitious materials for two-stage concrete," *J. Mater. Civ. Eng.*, vol. 29, pp. 04016298, 2017, http://dx.doi.org/10.1061/(ASCE)MT.1943-5533.0001841.

[74] S. Lee et al., "Effects of redispersible polymer powder on mechanical and durability properties of preplaced aggregate concrete with recycled railway ballast," *Int. J. Concr. Struct. Mater.*, vol. 12, 2018, http://dx.doi.org/10.1186/s40069-018-0304-1.

[75] H. F. Campos, N. S. Klein, J. Marques Filho, and M. Bianchini, "Low-cement high-strength concrete with partial replacement of Portland cement with stone powder and silica fume designed by particle packing optimization," *J. Clean. Prod.*, vol. 261, pp. 121228, 2020, http://dx.doi.org/10.1016/j.jclepro.2020.121228.

Author contributions: NTAS: conceptualization, experimental testing, data analysis, methodology, writing; GM: experimental testing, data analysis, writing; JHF: data analysis, supervision, writing; NSK: conceptualization, data analysis, supervision, writing.

Editors: Lia Lorena Pimentel, Daniel Carlos Taissum Cardoso.